



Neutron Imaging Detector Based on the μ PIC Micro-Pixel Gaseous Chamber



J.D. Parker, M. Harada¹, K. Hattori², S. Iwaki, S. Kabuki³, Y. Kishimoto⁴, H. Kubo, S. Kurosawa⁵, K. Miuchi, T. Oku¹, H. Nishimura, T. Sawano, T. Shinohara¹, J. Suzuki¹, T. Tanimori, K. Ueno⁶
Kyoto University, JAEA¹, UC Berkeley², Tokai University³, KEK⁴, Tohoku University⁵, RIKEN⁶

1. Introduction

We have developed a prototype neutron imaging detector which employs the micro-pixel gaseous chamber (μ PIC), a micropattern gaseous detector, coupled with a field programmable gate array (FPGA)-based data acquisition system for applications in small-angle neutron scattering and radiography at high-intensity neutron sources [1-3].

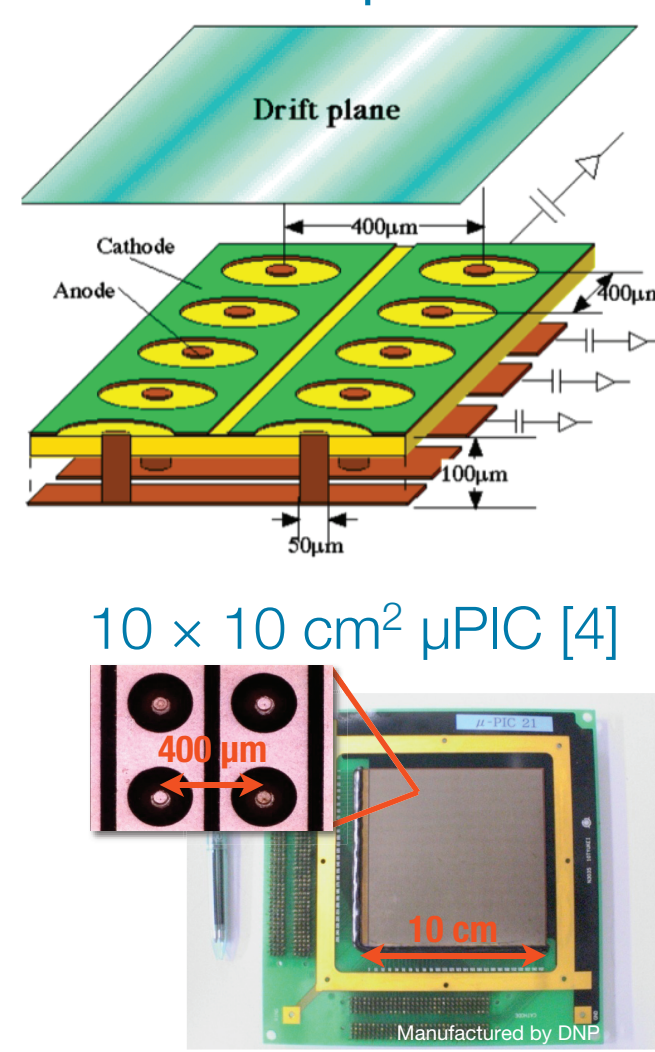
Features of our μ PIC-based detector

- Gas mixture of Ar-C₂H₆-³He (63:7:30) at 2 atm (current prototype).
- Large energy release for n-³He reaction (764 keV) requires low gas gain of <1000 (excellent stability against discharge).
- Detection efficiency up to 30% for thermal neutrons.
- Remains operable for more than 1 year on a single gas filling.
- Compact FPGA-based data acquisition system capable of high data rates (~10 MHz).
- Good spatial and time resolutions of <120 μ m and ~1 μ s, respectively.
- Strong rejection of gamma background (effective gamma sensitivity of <10⁻⁹).
- The μ PIC is available in sizes up to 30 x 30 cm² (larger areas accommodated by tiling).

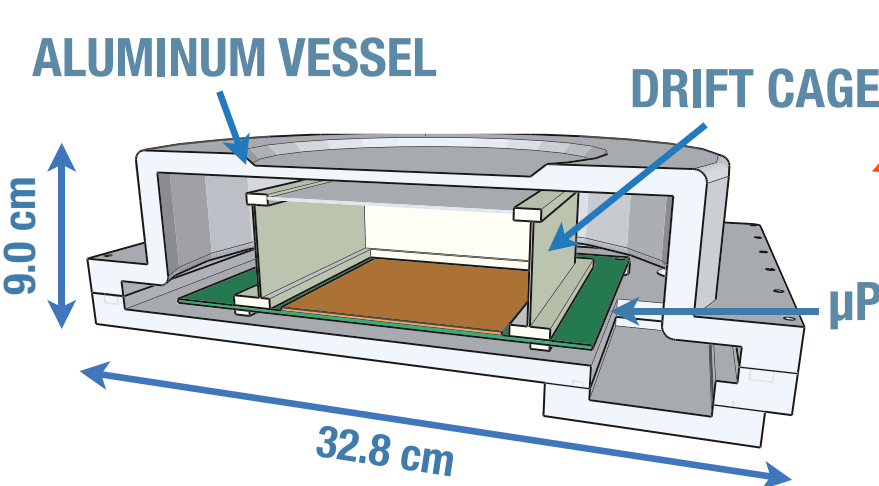
2. Prototype detector

The prototype detector uses a time projection chamber (TPC) consisting of an aluminum drift plane, drift cage, and a 10 x 10 cm² μ PIC. This TPC is contained within a 1-cm thick aluminum vessel that can accommodate drift heights up to 5 cm and is capable of withstanding pressures up to 2 atm. The μ PIC itself was developed in our group at Kyoto University [4] and is manufactured by DaiNippon Printing Co., Ltd., using inexpensive printed circuit board (PCB) technology.

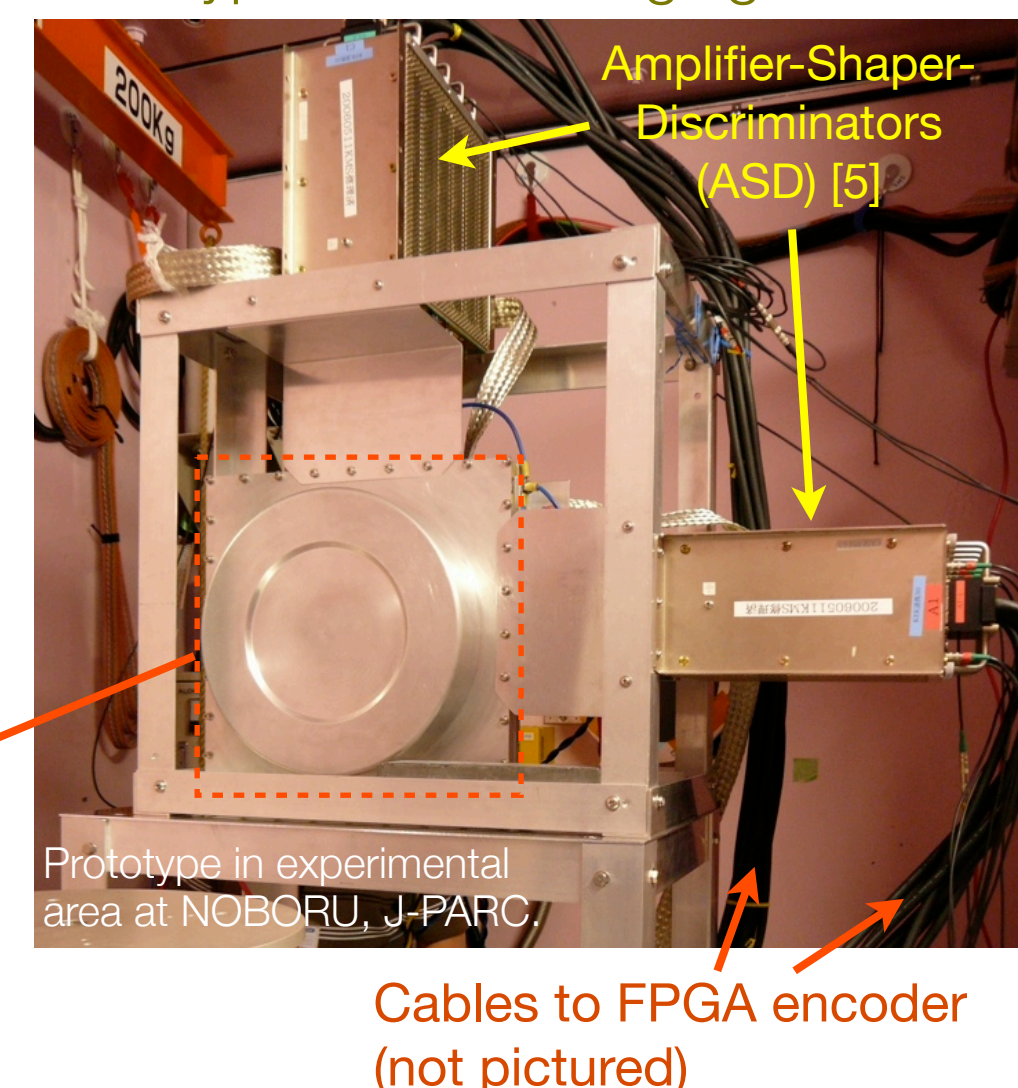
TPC with μ PIC



- 400- μ m pitch with 2D strip readout.
- 2D readout + drift-time gives 3D track.
- Low gain variation of ~4% (σ).
- Stable operation at gains up to 6000 (gain < 1000 needed for neutron imaging).



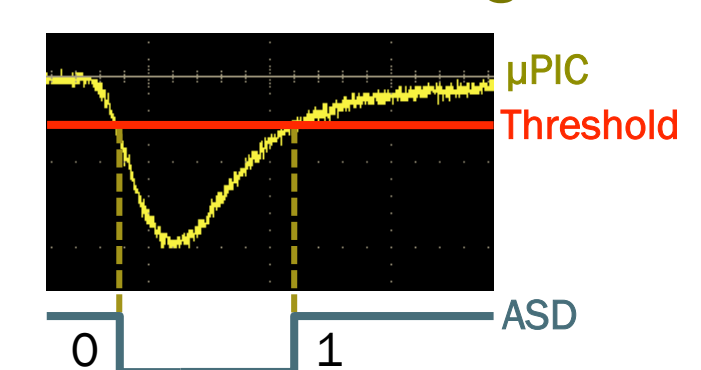
Prototype neutron imaging detector



3. FPGA encoder logic

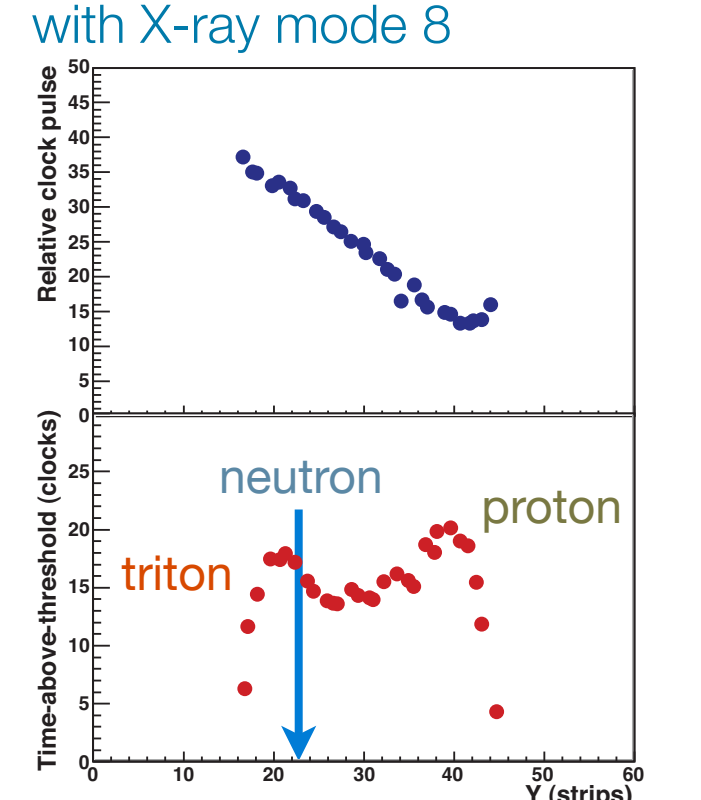
The heart of the data acquisition system (DAQ) is the FPGA encoder module [6]. The version of the FPGA firmware used for neutron imaging is known as X-ray mode 8. In this mode, all incoming data is streamed to the VME memory with no per-event trigger, and the individual events are later isolated in the offline analysis using a clustering algorithm. Additionally, by recording both the leading and trailing edge of the signals (new for mode 8), we are able to estimate the energy deposition using the time-above-threshold (TAT) method with no added cost or complexity for the DAQ.

Data encoding

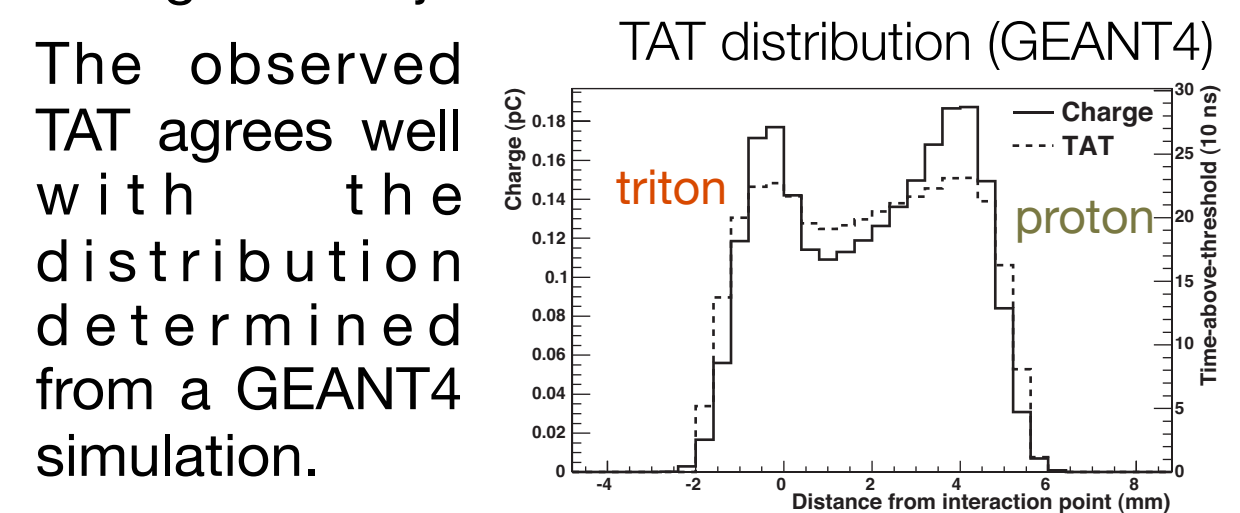


- Two data words per pulse (labeled 0 and 1).
- Time between words is proportional to energy deposit.

Proton-triton track measured with X-ray mode 8



Using the shape of the TAT distribution, we can separate the proton and triton (not possible by tracking alone) leading to improved position resolution and strong background rejection.



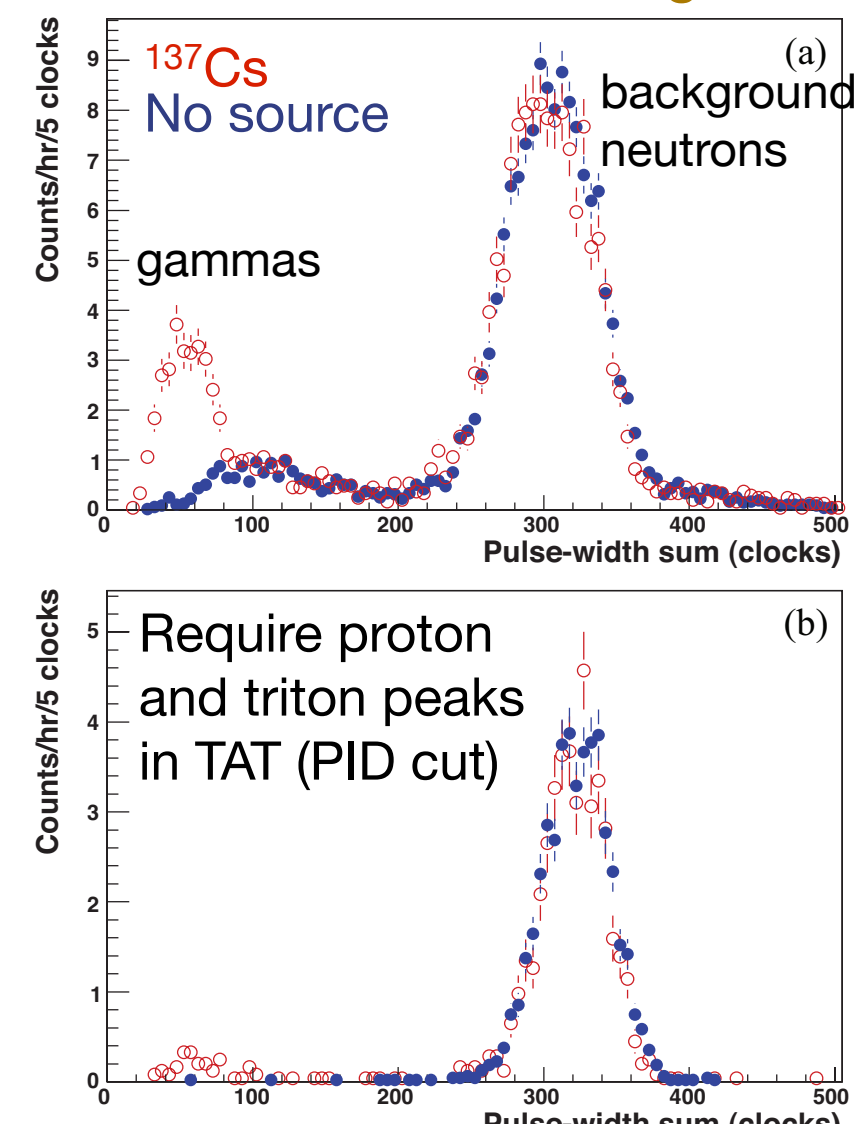
4. Detector performance

To study the performance of our prototype detector, three test experiments were carried out at the Japan Spallation Neutron Source (JSNS) located at the Japan Proton Accelerator Research Facility (J-PARC) in Tokai, Japan. The JSNS delivers a 25-Hz pulsed neutron beam to a total of 23 beam ports. Our measurements were carried out at NOBORU (NeutrOn Beamline for Observation and Research) [7], at beamline 10. The experiments were performed in Nov. 2009, June 2010, and Feb. 2011. Results for the first two experiments were reported in Refs. [2,3]. Additional tests were performed at our laboratory using various radioisotope sources. For all of the measurements described below, the detector was filled with a gas mixture of Ar-C₂H₆-³He (63:7:30) at 2 atm.

4.1. Neutron-gamma separation

Neutron-gamma separation is achieved by combining information about the energy deposition (via time-above-threshold) and track length. Neutrons produce proton-triton tracks with essentially the same energy and track lengths, while gamma events deposit much less energy and produce a range of track lengths. The gamma rejection capability of the prototype was studied using a 1-MBq ¹³⁷Cs source, which produces gamma-rays at an energy of 662 keV.

TAT sum after track-length cut



- Neutron track-length determined from data (~7.6 mm for present data set).
- TAT sum > 140 to select neutrons.
- PID cut selects events with double-peak structure associated with proton and triton Bragg peaks.

After subtracting the background counts determined from the no-source data, upper limits for the gamma contamination were found to be < 9.3 x 10⁻⁶ and < 3.6 x 10⁻⁶ (95% CL) for the data in plots (a) and (b), respectively. When combined with the gamma detection efficiency (~10⁻³), this gives an effective gamma sensitivity on the order of 10⁻⁹ or less.

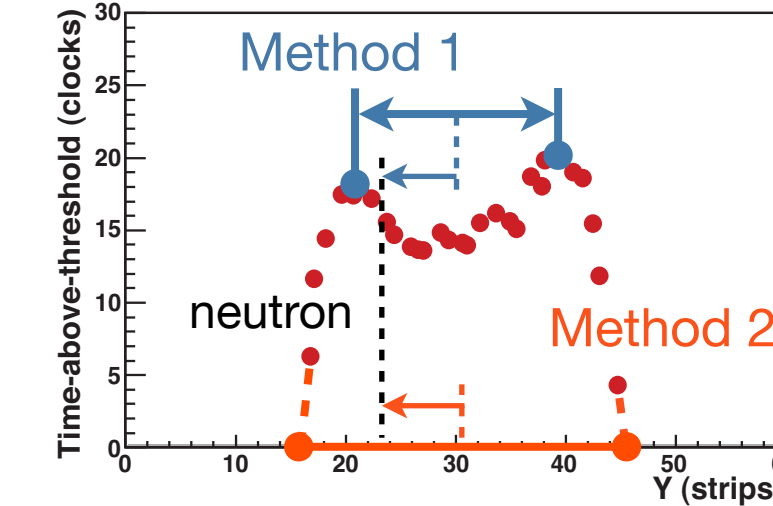
Gamma contamination. Data is in counts/hr.

Cuts	¹³⁷ Cs	No source
None	351363 ± 120	3700.4 ± 8.8
Track length	185.0 ± 2.7	161.1 ± 1.8
+ TAT sum	145.6 ± 2.4	148.7 ± 1.8
+ PID	43.4 ± 1.3	46.1 ± 1.0

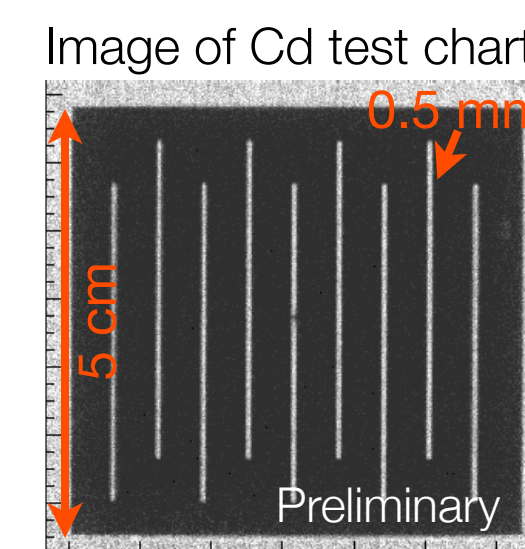
4.2. Position resolution

To determine the neutron interaction position for a particular event, we need to know two things: 1) the width of the track in x and y, and 2) the proton direction (both are determined from the shape of the TAT distribution). Once these are known, a correction can be made from the mid-point of the track to the estimated neutron interaction position. The position resolution was studied at NOBORU in Feb. 2011 using a cadmium test chart with a slit pattern consisting of 0.5-mm slits at a pitch of 5 mm. The detector was placed in the neutron beam at distance of 14.5 m from the moderator, and the test chart was attached directly to the front of the vessel.

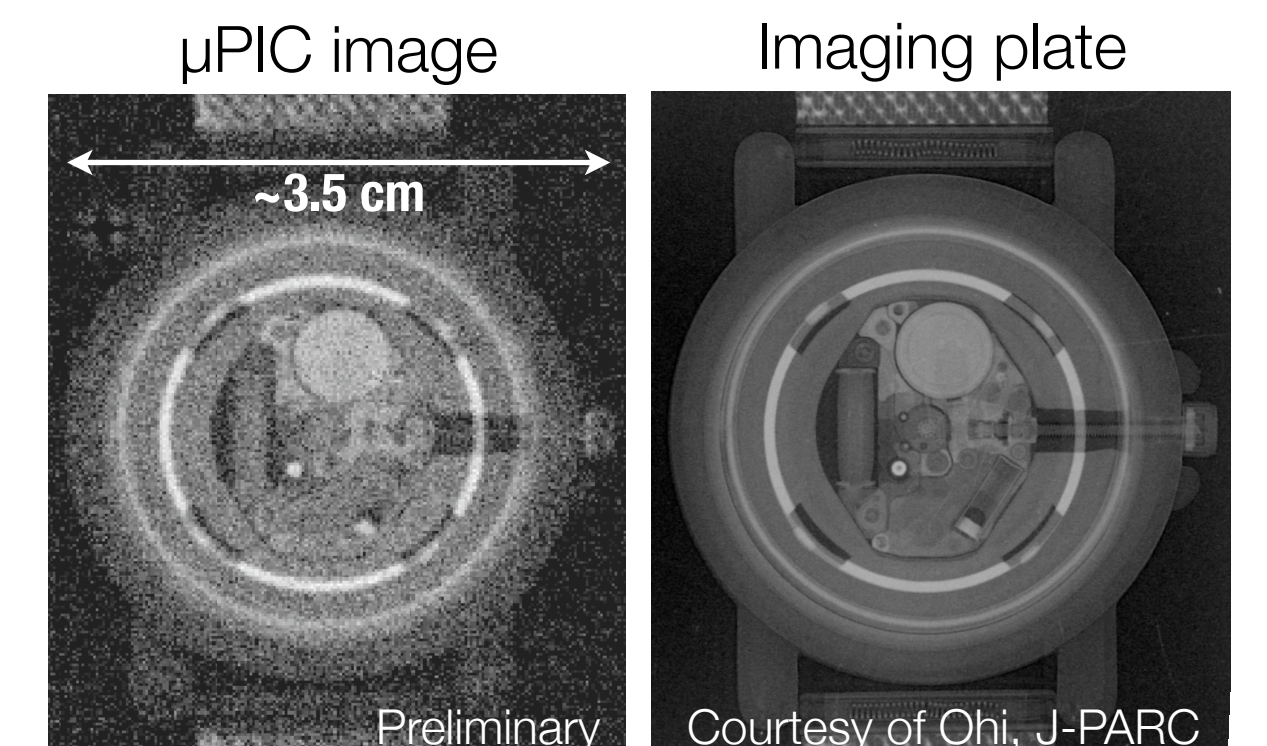
Track width from TAT distribution



- Peak interpolation (method 1) gives track width as distance between Bragg peaks of proton and triton.
- End-point extrapolation (method 2) uses the shape of the distribution to extrapolate to zero.
- Offsets to neutron position were determined with the aid of our GEANT4 simulation and the real data.



The final neutron position was determined by the weighted average of methods 1 and 2. Using the image of the Cd test chart (left), the resolution was determined at each slit and averaged to obtain the final value of $\sigma = 116.3 \pm 0.5 \mu$ m (an improvement of nearly a factor of 3 over the previous determination [3]).



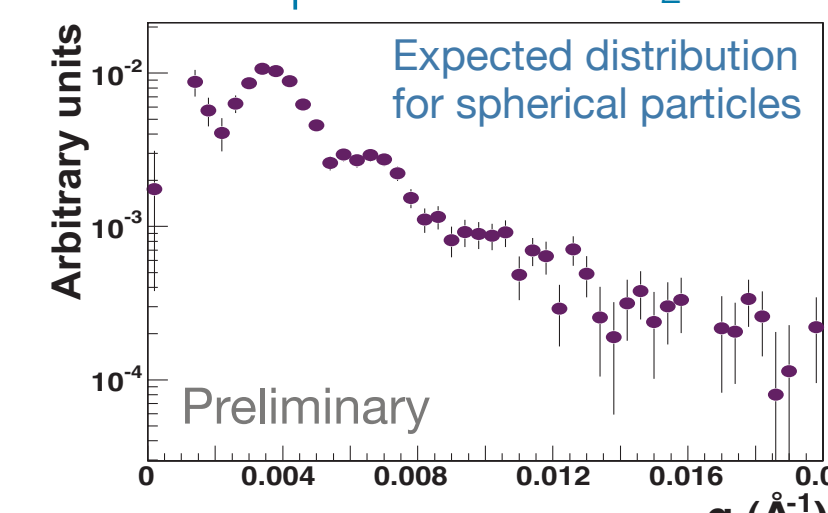
4.3. Long-term operability

At a time when the global demand for ³He is outstripping the world's supply [8], it is important to minimize the ³He usage of our detector. In our sealed detector, the build-up of impurities over time leads to a degradation in the properties of the gas. Thus, to maintain the desired gas properties, the detector must be periodically evacuated and refilled. Over the course of testing, we found that the detector remained operable for more than one year on a single gas filling. Several strategies can be employed to further increase the time between gas fillings: 1) annealing of the vessel and μ PIC to reduce outgassing, and 2) a gas filtration system to remove any impurities that build up in the gas. If these are realized, the operation cycle of the detector could be extended almost indefinitely, greatly reducing maintenance costs related to ³He gas.

5. Demonstration measurements

Several demonstration measurements were made at NOBORU in Nov. 2009 (SANS) and Feb. 2011 (resonance absorption, Bragg-edge transmission).

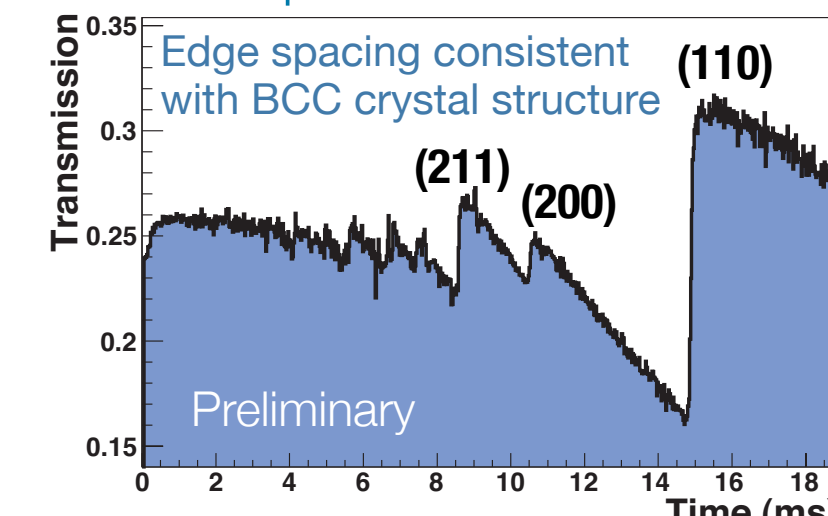
1. SANS pattern for SiO₂



1. SANS (J-PARC, Nov. 2009)

Sample: spherical SiO₂ nanoparticles (diameter ~200 nm). Detector-to-sample: 1666 mm. Exposure time: 35 min.

2. Bragg-edge transmission for Fe powder

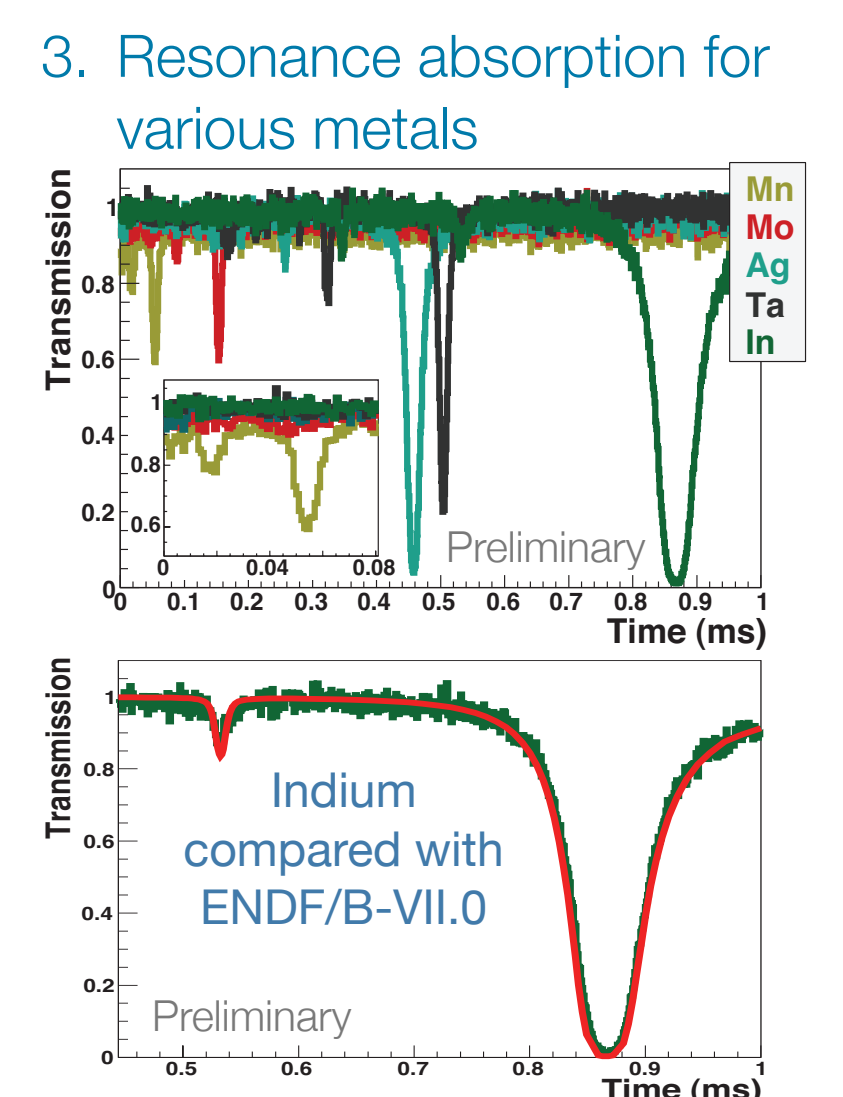


2. Bragg-edge transmission (J-PARC, Feb. 2011)

Sample: Fe powder (grain size <325 μ m, sample thickness of 1.6 cm). Exposure time: 40 min.

3. Resonance absorption for various metals

Samples: Mn, Mo, Ag, Ta, and In sheets (typical area of 10 x 10 cm², thicknesses from 0.01 to 1.0 mm). Exposure time: ~16 min/sample.



6. Future improvements

Currently, efforts to optimize the gas mixture for improved position resolution of the detector are underway. For instance, by switching the quencher gas to CO₂, we expect diffusion to be greatly reduced, resulting in a position resolution of ~100 μ m (estimated using MAGBOLTZ and GEANT4). Further reductions can be obtained by reducing the pixel pitch of the μ PIC. By rearranging the anode pixels (dense packing), we can reduce the pixel pitch, and, thereby, improve the position resolution, by as much as another 30%.

For the DAQ, an ultra-compact encoder, which combines new low-power discriminator chips and an FPGA on a single board, has recently been developed in our group. In addition to significantly reducing the bulk of the system, the new encoder is expected to achieve data rates about 5 times higher than the current encoder system.

7. Conclusion

By measuring both the energy deposition (via time-above-threshold) and track positions, a position resolution of <120 μ m and an effective gamma sensitivity of <10⁻⁹ were achieved. The time resolution of ~1 μ s, as determined by the electron drift velocity, enables clean separation of neutrons by time-of-flight at pulsed neutron sources. The detector operates at a moderate pressure of a few atmospheres and is able to maintain its good operating characteristics for more than one year on a single gas filling. The compact, high-speed FPGA-based DAQ is simple to setup and operate and is capable of data rates of ~10 MHz. Furthermore, the printed circuit board manufacturing process is inexpensive and allows for freedom in choosing the size and shape of the μ PIC (up to 30 x 30 cm², with larger areas accommodated by tiling). These properties make the μ PIC an attractive solution for neutron imaging applications in high-rate environments that require very low background, time-resolved measurements and the ability to cover large areas at moderate resolution.

References

- T. Tanimori et al., Nucl. Instr. and Meth. A 529 (2004) 236.
- J.D. Parker et al., 2009 IEEE Nuclear Science Symposium Conference Record (©2009 IEEE) 1107.
- J.D. Parker et al., 2010 IEEE Nuclear Science Symposium Conference Record (©2010 IEEE) 291.
- A. Ochi et al., Nucl. Instr. and Meth. A 471 (2001) 246.
- R. Orito et al., IEEE Trans. Nucl. Sci., 51 (2004) 1337.
- H. Kubo et al., 2005 IEEE Nuclear Science Symposium Conference Record (©2005 IEEE) 371.
- F. Maekawa et al., Nucl. Instr. and Meth. A 600 (2009) 335.
- R.T. Kouzes, The ³He Supply Problem, Technical Rpt. PNNL-18388, Pacific Northwest National Laboratory, Richland, WA (2009).